

The Numerical Evaluation of a SAR Measurement Phantom at the Telstra Research Laboratories

Robert L McIntosh, Ray McKenzie, and
Amico Carratelli

Electromagnetic Energy Safety Research, Telstra Research Laboratories,
770 Blackburn Rd, Clayton, Victoria, Australia, 3168
email: robert.l.mcintosh@team.telstra.com

Abstract – At Telstra Research Laboratories (TRL), both experimental and computational environments have been established to determine the levels of electromagnetic energy (EME) induced in the human body from exposure to radiofrequency (RF) transmitters.

The experimental facilities feature a robot controlled measurement system, and a set of fibreglass human phantoms that can hold various human tissue equivalent liquids. A phantom can be exposed to an RF source under investigation, and the interior of the phantom scanned by the robot to determine the localised specific energy absorption rate (SAR). Measurement of the SAR level is presently the standard method of showing compliance with regulatory RF safety limits.

The computational modelling environment complements the experimental approach. Numerical models of the human body can be used for prompt evaluation of SAR levels under a wide range of scenarios that may not be easily achieved experimentally. This paper discusses the development of numerical models of the phantom and their use to evaluate the accuracy of the experimental approach.

Introduction

At TRL, evaluations are performed on exposures produced by RF sources such as mobile phones, hands-free technologies, and mobile radio network infrastructure. Evaluations are also made on the efficacy of various mobile phone shields and other add on accessories.

To undertake experimental research on EME exposure, TRL has developed a robotically controlled SAR measurement system (see Figure 1). The system consists of a robot, a set of miniature implantable isotropic electric (E) field probes, a set of fibreglass human phantoms, various human tissue equivalent liquids (developed following the methods of Hartsgrrove et al. [9]) and associated control instrumentation and software. The dielectric properties of the liquids, which fill the interior of the phantom, simulate the aggregate properties of human tissues at the frequency of interest as described in the work of Hurt, Gabriel and others [8, 10] or as

prescribed in the test protocols of the regulating authorities [3]. A detailed discussion of the development of the robot, usage and measurement techniques, and its use in a study of mobile phone hands free kits, is presented in [13].

The experimental facilities at TRL are complemented through the establishment of a computational modelling environment, including semi-analytical and finite-difference software packages, that can be used for the analysis of EME exposure.

It is generally accepted that SAR is the most appropriate metric for determining EME exposure in the very near field of a RF source [1, 4]. In both the experimental and computational environments, the SAR (W/kg) can be determined at any point from the E-field (V/m) (measured or calculated) at that point by:

$$SAR = \frac{\sigma |E|^2}{\rho}$$

where σ is the conductivity ($\Omega^{-1}\text{m}^{-1}$) of the tissue in which the measurement is made and ρ is its mass density (kg/m^3).

The point SAR data must be further processed to obtain the required mass averaged SAR. In Australia, the Australian Communications Authority (ACA) sets the averaging mass to be 1 g of tissue in the shape of a cube [3]. Since the density of most biological tissues is generally close to $1000 \text{ kg}/\text{m}^3$, this equates to a volume of around 1 cm^3 . 10 g of tissue, another common averaging mass, equates to a cube of approximately 2.15 cm in length.

In this paper a description is given of the development of a finite-difference numerical model of the experimental phantom used at TRL. This model provides the capacity to verify the accuracy and effectiveness of experimental analyses.

A comparison is also provided of a numerical model of the phantom's head and a detailed numerical head model complete with different tissue types (developed by Remcom Inc. [15]).

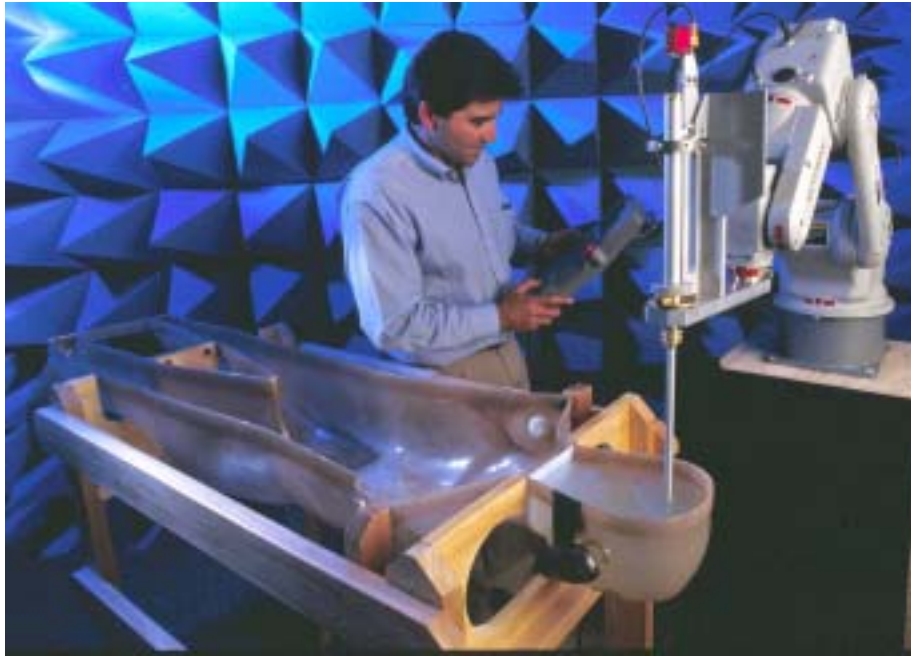


Figure 1. The SAR Robot Measurement System at TRL

FDTD Model of the Phantom

The company Remcom Inc., produces electromagnetic (EM) simulation software [15]. Their product XFDTD is an EM solver based on the Finite Difference Time Domain (FDTD) method. The package has many features including a graphical user interface, and the capability to calculate SAR distributions, peaks and averages. Plane waves, or voltage and current sources can be used to excite a specified structure. An important aspect of an FDTD model is the use of a mesh of cells to simulate the physical structure under analysis. (For a description of the FDTD method, see, for example, reference [12].)

The first step in creating a mesh of the phantom was the mapping of the geometrical shape of the fiberglass shell. This data was used to determine the outermost cell vertices of the mesh. For the head, the distance from each of these vertices to the fiberglass shell is no more than 2 mm. A full three-dimensional mesh was then obtained by filling in all the inner cubical cells. A two-dimensional slice of the head mesh is shown in Figure 2. The fiberglass structure and other surrounding materials are ignored. Separate meshes were created for the phantom's head and torso. These can be combined if required.

In this paper, the XFDTD models of the phantom consider the electromagnetic excitation to be

- 900 MHz plane wave
- EHK polarisation (that is, propagation from the front to the back of the head, and the E-field polarised in the vertical direction)
- incident power density of 10 W/m^2

The phantom head is homogeneous with the electrical properties

- conductivity $0.77 \text{ } \Omega^{-1}\text{m}^{-1}$
 - relative permittivity 45.8
- and mass density
- 1060 kg/m^3

These electrical properties are those described in [7, 8] for the human brain (an average for both white and grey matter).



Figure 2. 2 mm Mesh of the Phantom's Head

Cell Size Evaluation

In a finite difference analysis, a compromise is often needed between the number of cells (which directly influences the model run-time) and the accuracy required.

The XFDTD manual [16] suggests that in the region between the head geometry and the outer mesh boundary (comprised of air) there should be at least fifteen cells or one-third of a wavelength if the cell size is small relative to the wavelength. For models considered in this paper both of these conditions were satisfied. A full mesh consists of 558,000 cells when cells of 5 mm in length are used; over 12 million cells are needed when 1.75 mm cells are used.

The manual also indicates “The cell edges must be smaller than approximately one-tenth of a wavelength for accurate results.”. At 900 MHz the wavelength in free space is 333 mm in length. With a relative permittivity of 45.8 for the phantom head the wavelength reduces to 49 mm (this effect can be seen in Figure 3). This equates to choosing a cell size of no more than 4.9 mm.

An analysis was performed to test this recommendation using models with cells ranging from 1.75 mm in length to models with cells 5 mm in length. The results are presented in Table 1. Two-dimensional profiles of the centerline slice are presented in Figure 3 for the models with 2 mm and 5 mm cells.

For all five models, the whole head average SAR values are in close agreement. The profiles are also very similar (including those shown in Figure 3).

However, there is a considerable variation with both the peak 1 g and 10 g values. (The peak values were recorded near the upper ridge of the nose.) In particular, consistent values (within 8%) are not obtained until the cell size is 3 mm or below.

Table 1. Influence of Cell Size

cell length (mm)	whole head average SAR (W/kg)	peak 1 g SAR (W/kg)	peak 10 g SAR (W/kg)
5.00	0.088	0.74	0.59
4.00	0.090	0.79	0.49
3.00	0.090	0.91	0.59
2.00	0.090	0.99	0.63
1.75	0.090	0.94	0.63

Thus, for the phantom head, a suitable compromise is a model with cells of length 2 mm (for a total of eight million cells). The run-time is around five hours (on a HP C240 workstation).

The results also produce a similar conclusion to that presented in [5] (where the focus was 60 Hz fields) that “... higher resolution modeling generally predicts peak electric fields intensities ... that are slightly higher than those computed using lower resolution modeling.”. This is an important consideration if modeling is used to determine peak SAR values.

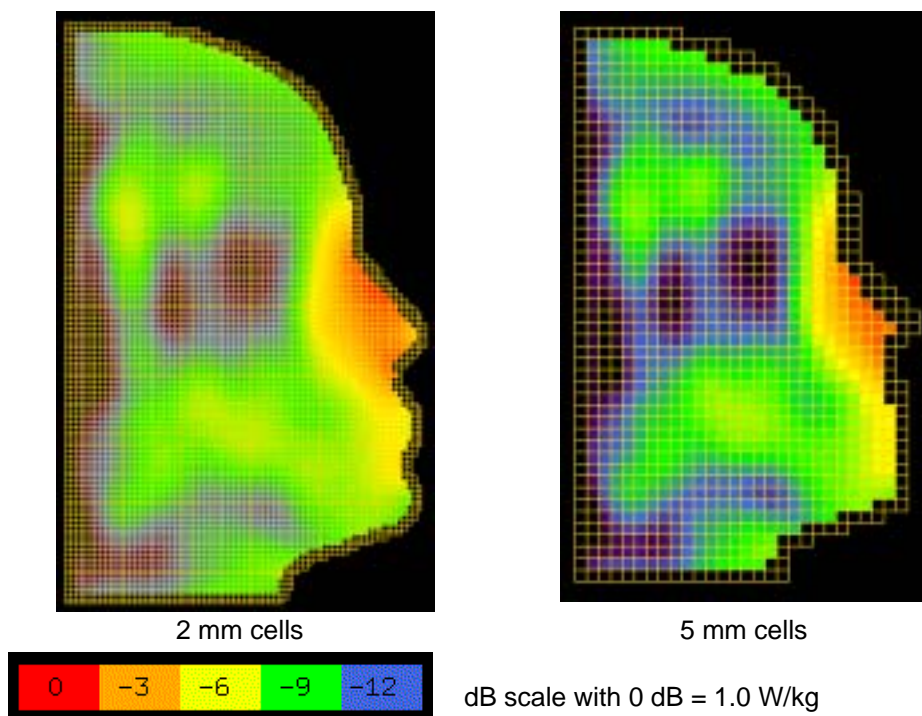


Figure 3. Comparison of the 1 g SAR profiles for 2 mm cell and 5 mm cell models of the Phantom

Comparison of the TRL Phantom with the Visible Human

Sophisticated full body models have recently been developed that include the discrimination of various tissue types, something that is difficult to provide in an experimental setup. In particular, the Remcom company has produced human body meshes that are derived from the Visible Human project (for details see, for example, the site http://www.nlm.nih.gov/research/visible/visible_human.html). For examples of full body models from other research organizations see [6, 14].

A two-dimensional slice through the mesh of the Visible Human head is shown in Figure 4 (the length of each cell is 2 mm). Different colours in the figure represent various tissue types - their electrical and material properties are presented in Table 2.

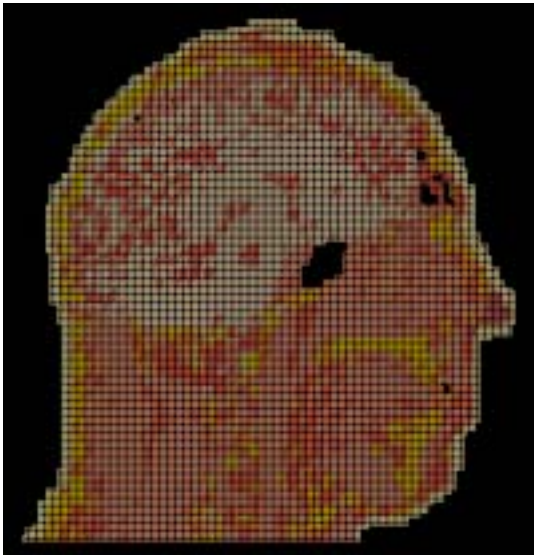


Figure 4. XFDTD model of the head of the Visible Human

Table 2. Head Tissue Properties (electrical properties for 900 MHz)

tissue	conductivity ($\Omega^{-1}\text{m}^{-1}$)	relative permittivity	mass density (kg/m^3)
cartilage	0.782	42.65	1000
muscle	0.969	55.95	1050
eye	1.900	70.00	1000
brain & nerve	0.766	45.80	1050
dry skin	0.867	41.40	1000
blood	1.180	62.00	1000
skull	0.242	16.62	1850

Note: these values are the set values given in the XFDTD package and may differ from those in [7, 8].

For this paper, the Visible Human body mesh has been normalised so that the height of the body is 1.77 m high. This is in line with values for the ICRP 'reference man' [11 p189]. The resultant normalised head is 264 mm high, 176 mm wide, and 240 mm deep. The head of the TRL phantom is smaller at 236 mm high, 166 mm wide, and (with the back of the head not present) the depth is 146 mm.

Figure 5 presents two-dimensional slices of results given by the XFDTD analysis of the Visible Human model and the phantom model. A homogeneous version of the Visible Human model is also presented (using the same electrical and material properties of the phantom). All models have 2 mm cells.

In response to the propagation direction of the exciting field (that is, from front-to-back), the highest SAR values are concentrated around the nose and chin of the models.

The first observation is the overall similarity between the three models giving us confidence in using the TRL phantom head for experimentation. However, the differences that there are between the models highlight the significant factors that need to be considered when evaluating the experimental results.

In the Visible Human model the peak SAR is at the base of the nose. This peak coincides with a sharp turn between nose and upper lip and also with the presence of the higher conductivity tissues – skin, blood, and cartilage. Blood in the chin region also coincides with moderately high SAR values. The presence of skin around the models also differentiates the Visible Human from the homogeneous models.

In the phantom model the peak SAR is along the top ridge of the nose. This difference with the Visible Human appears to be for geometrical reasons. The nose is slightly longer than the Visible Human model and the angle between the nose and the forehead is slightly larger. The base of the nose is also slightly rounder.

Table 3 indicates the average and peak SAR values for the three models, providing a quantitative comparison.

Table 3. SAR values for Phantom and Visible Human models (2 mm cells)

model	head avge. SAR (W/kg)	1 g peak (W/kg)	10 g peak (W/kg)
Phantom	0.090	0.99	0.63
Visible Human	0.078 * 0.065 **	1.04	0.61
Visible Human homogeneous	0.076 * 0.063 **	0.73	0.53

* to the same depth as the phantom head

** for the whole head

Comparing the Visible Human model with its homogeneous version, we observe that the average SAR values are similar. However, the 1 g peak SAR is significantly higher in the (heterogeneous) Visible Human model (around 42% higher). This is due to the presence of high conductivity tissues (blood, skin, and cartilage) in the vicinity of the nose. For further comparisons of homogeneous and heterogeneous models see references [17, 18] (where mobile phones are used as the source). In [18] it is found that "... homogeneous modeling may result in an underestimate [of] about 20% ..." in peak SAR.

The 1 g peak for the TRL phantom is a similar amount (36%) higher than the homogeneous version of the

Visible Human. This, however, is due to the difference in head shape.

The combination of the influence of material conductivities and the geometry therefore have the coincidental effect that the 1 g peak SAR for the phantom and the Visible Human model are in close agreement (within around 5%).

It should finally be noted that the average (rather than peak) SAR for the phantom is significantly higher than that for the Visible Human models. The different head shapes (in particular the longer nose in the Phantom) seems to be the main factor.

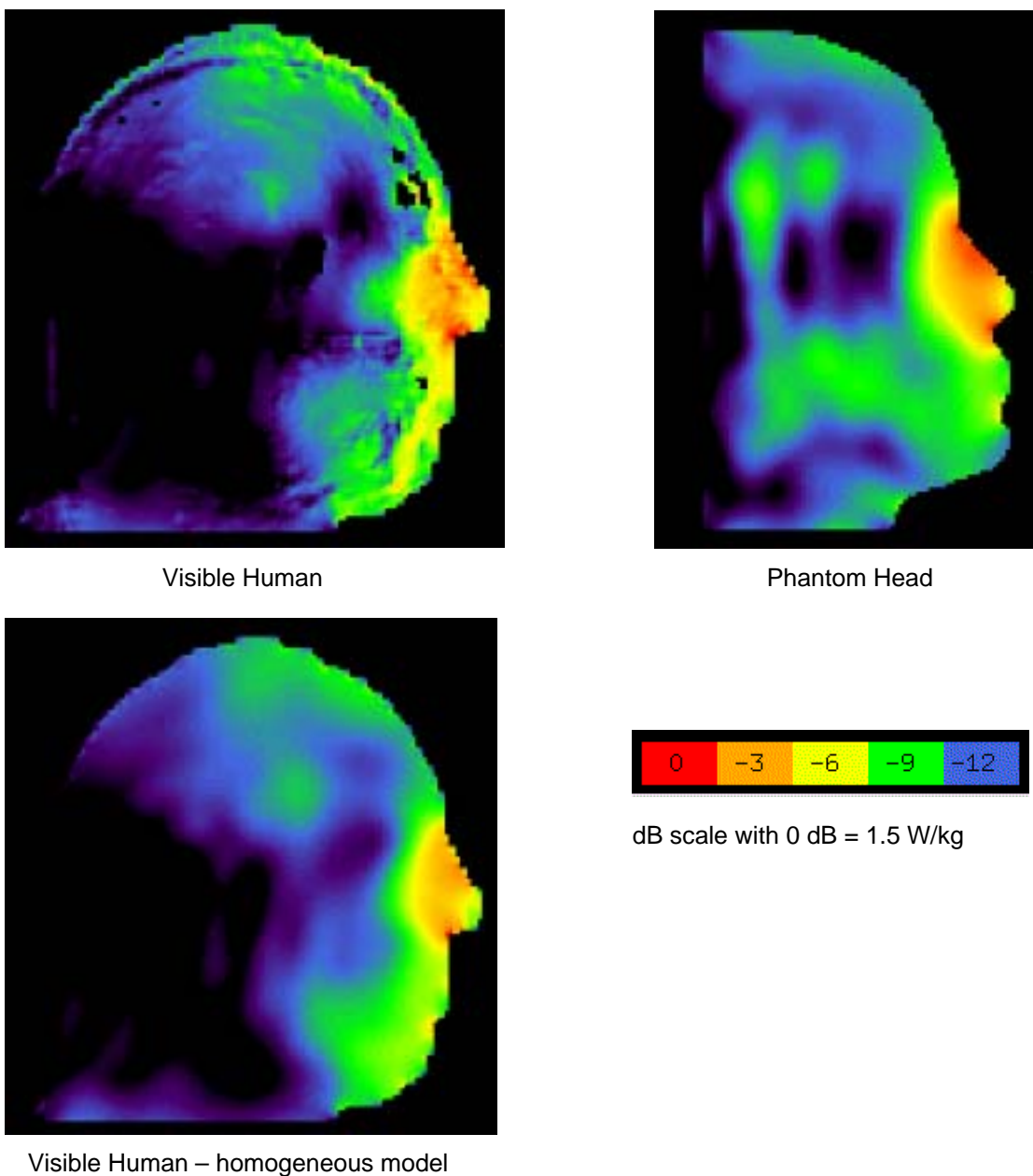


Figure 5. Comparison of the Phantom head and the Visible Human head

Conclusions

At Telstra Research Laboratories, both experimental and computational environments have been established to examine levels of electromagnetic power dissipated in the human body from exposure to radiofrequency sources such as mobile phones and mobile radio network infrastructure.

This paper describes the development of a finite difference numerical model of the TRL physical phantom (that is used in the experimental setup). This model provides the capacity to verify the accuracy and effectiveness of experimental analyses.

The evaluation of the cell size showed that all models of the head, with cells of length 5 mm or below, had similar profiles and average SAR (for a 900 MHz plane-wave excitation). However, the 1 g peak and 10 g peak values increased with higher mesh resolution, not converging to the maximum values until the cell length reduced to 2 mm.

A comparison was provided of the phantom head model with a detailed human head model complete with different tissue types (developed by Remcom Inc. [15]), and also with the human head model with homogeneous material properties. The results indicated the significant influence of various tissue types and body shape, important factors when interpreting experimental results. In particular, (for a 900 MHz plane wave excitation) the whole head average SAR for the phantom is significantly higher than for the human head models (whilst the peak values are of similar magnitude). Also, peak SAR values are significantly higher for the heterogeneous human head model than for the homogeneous version.

References

1. Allen S G, "Radiofrequency field measurements and hazard assessment", *Journal of Radiological Protection*, Vol II-1, 1996.
2. ANSI/IEEE, "IEEE Standard for Safety Levels with Respect to Human Exposure to Radio Frequency Electromagnetic Fields, 3 kHz to 300 GHz", ANSI/IEEE C95.1-1992 (see <http://standards.ieee.org/cgi-bin/status>), 1992
3. Australian Communications Authority, "Radiocommunications (Electromagnetic Radiation – Human Exposure) Standard", Schedule 1, Test Method, "Specific Absorption Rate Test Method Using Phantom Model of Human Head (1): 1998", 1999.
4. Chou C K, Bassen H, Osepchuk J, Balzano Q, Peterson R, Meltz M, Cleveland R, Lin J C and Heynick L, "Radio Frequency Electromagnetic Exposure: Tutorial Review on Experimental Dosimetry," *Bioelectromag.*, Vol 17, No 3, 1996.
5. Dawson T W, Caputa K, and Stuchly M A, "Influence of Human Model Resolution on Computed Currents Induced in Organs by 60-Hz Magnetic Fields", *Bioelectromag.*, 18, 1997, pp478-490.
6. Dimbylow P J, "FDTD Calculations of the Whole-Body Averaged SAR in an Anatomically Realistic Voxel Model of the Human Body from 1 MHz to 1 GHz", *Phys. Mde. Biol.* 42, 1997, pp 479-490.
7. Federal Communications Commission (FCC), <http://www.fcc.gov/fcc-bin/dielec.sh>, FCC web site on Tissue Dielectrics.
8. Gabriel C, "Compilation of the Dielectric Properties of Body Tissues at RF and Microwave Frequencies", Brooks Air Force Base, report no. AL/OE-TR-1996-0037, 1996.
9. Hartsgrove G, Kraszewski A, Surowiec A, "Simulated Biological Materials for Electromagnetic Radiation Absorption Studies", *Bioelectromag.*, Vol 8, 1987.
10. Hurt W D, "Radiofrequency Radiation Dosimetry Workshop", Brooks Air Force Base report no. AL/OE-SR-1996-0003, 1996.
11. ICRP, "Human Respiratory Tract Model for Radiological Protection: A Report of Committee 2 of the ICRP", ICRP Publication 66, 1994.
12. Kunz K S, and Luebbers R J, "The Finite Difference Time Domain Method for Electromagnetics", CRC Press, 1993.
13. McKenzie R, Garcia-Webb M, Carratelli A, Anderson V, and Armstrong M, "The Development and Application of a SAR Robot at the Telstra Research Laboratories", *Proceedings of The 2nd Conference of the Victorian Chapter of the IEEE Engineering in Medicine and Biology Society, Biomedical Research in 2001*, held at Monash University, Clayton, Victoria Australia, February 19-20, 2001, pp 179-182.
14. Mason P A, Ziriak J M, Hurt W D, Walters T J, Ryan K L, Nelson D A, Smith K I, and D'Andrea J A, "Recent Advancements in Dosimetry Measurements and Modeling", *Radio Frequency Radiation Dosimetry*, Kluwer Academic Publishers, 2000, pp 141-155.
15. Remcom, Inc. website <http://www.remcom.com>.
16. Remcom, Inc., "User's Manual for XFDTD; The Finite Difference Time Domain Graphical User Interface for Electromagnetic Calculations", Ver 5.0.4.9, Sept 1999, available from [15].
17. Riu P J, Foster K R, "Heating of Tissue by Near-Field Exposure to a Dipole: A Model Analysis", *IEEE Transactions on Biomedical Engineering*, Vol 46, No 8, 1999, pp911-917.
18. Wang J, and Fujiwara O, "The Role of Head Tissue Complexity in the Peak SAR Assessment for Mobile Phones", *EMC 2000 International Wroclaw Symposium on Electromagnetic Compatibility*, pp255-259.

